



OPEN Zinc finger protein 263 promotes colorectal cancer cell progression by activating STAT3 and enhancing chemoradiotherapy resistance

Yadan Du^{1,3,4}, Yawen Chen^{1,3,4}, Zaihua Yan^{2,4}, Jian Yang³ & Mingxu Da^{1,3}✉

Zinc finger protein 263 (ZNF263) is frequently upregulated in various tumor types; however, its function and regulatory mechanism in colorectal cancer (CRC) have not yet been elucidated. In this study, the expression of ZNF263 was systematically examined using data from The Cancer Genome Atlas database and samples from patients with CRC. The results indicated that high expression of ZNF263 in CRC tissues is significantly associated with tumor grade, lymph node metastasis and distant metastasis. Additionally, overexpression of ZNF263 significantly promoted the proliferation, invasion, migration, and epithelial-mesenchymal transition of CRC cells, while also increasing signal transducer and activator of transcription 3 (STAT3) expression and mRNA stability. Conversely, knockdown of ZNF263 inhibited the malignant behavior of CRC cells and decreased STAT3 expression and mRNA stability. Further mechanism studies using chromatin immunoprecipitation (CHIP) and luciferase assays verified that ZNF263 directly binds to the STAT3 promoter. Rescue experiments demonstrated that the knockdown or overexpression of STAT3 could significantly reverse the effects of ZNF263 on CRC cells. Additionally, our study found that overexpression of ZNF263 enhanced the resistance of CRC cells to the chemoradiotherapy. In summary, this study not only elucidated the significant role of ZNF263 in CRC but also proposed novel approaches and methodologies for the diagnosis and treatment of this malignancy.

Keywords Colorectal cancer, Zinc finger protein 263, Signal transducer and activator of transcription 3, Radiotherapy, Chemotherapy, Epithelial-mesenchymal transition

Colorectal cancer (CRC) is a major malignancy of the digestive system and a major cause of cancer-related mortality¹. Often asymptomatic in its early stages, CRC is frequently diagnosed at an advanced stage, complicating treatment efforts. While surgical resection remains the most effective treatment for early and locally advanced CRC, its efficacy diminishes significantly in advanced and metastatic cases, necessitating the use of multimodal therapies². In recent years, immune checkpoint inhibitors have become essential in the first-line treatment of advanced and metastatic CRC, particularly in patients with mismatch repair (MMR) deficiencies or high microsatellite instability (MSI-H). However, their effectiveness is limited in microsatellite-stable (MSS) CRC, highlighting the need for alternative strategies. The challenges posed by tumor heterogeneity, drug resistance, and immune escape mechanisms further underscore the importance of continued research into the molecular mechanisms of CRC^{3,4}. Consequently, identifying novel targets and optimizing combination therapies are critical to overcoming current limitations and improving patient outcome.

Transcription factors known as zinc finger proteins (ZNFs) have the ability to bind to certain DNA sequences and control the expression of target genes^{5,6}. For instance, in hepatocellular carcinoma (HCC) cells, ZNF263 and myelin transcription factor 1-like form a complex that supports cell growth and enhances metastatic potential, thereby worsening the malignancy of HCC⁷. Moreover, ZNF263 has demonstrated similar oncogenic effects in various other cancer types. Specifically, the upregulation of ZNF263 in kidney cancer⁸, glioblastoma⁹ and non-small cell lung cancer¹⁰ cells has been linked to increased cell proliferation and enhanced resistance to chemotherapeutic agents. Additionally, ZNF263 promotes epithelial-mesenchymal transition (EMT) and drug resistance in pancreatic cancer by activating ring finger protein 126 (RNF126)¹¹. These findings suggest

¹The First School of Clinical Medicine, Gansu University of Chinese Medicine, Lanzhou 730000, China. ²The Second Department of Gastrointestinal Surgery, The Affiliated Hospital of North Sichuan Medical College, Nanchong 637000, China. ³Department of Surgical Oncology, Gansu Provincial Hospital, Lanzhou 730000, China. ⁴Yadan Du, Yawen Chen and Zaihua Yan contributed equally to this work. ✉email: ldy_damx@lzu.edu.cn

that ZNF263 could serve a pivotal role in various tumor types, influencing tumor development, EMT and chemotherapy resistance. However, despite these insights, the precise role and impact of ZNF263 in CRC remain poorly understood, which highlights a critical gap in the current understanding of CRC pathophysiology and underscores the need for further research.

Signal transducer and activator of transcription 3 (STAT3) has a crucial role in CRC development and progression. As a key transcription factor, the aberrant activation of STAT3 is closely related to the pathophysiological processes of a number of cancer types, particularly CRC. STAT3 regulates various cancer-related biological processes, such as cell proliferation and apoptosis, angiogenesis and immune escape, by modulating the expression of downstream target genes^{12–14}. Additionally, persistent activation of STAT3 is strongly associated with poor prognosis in patients with CRC, making it a potential therapeutic target¹⁵. Furthermore, STAT3 significantly contributes to chemoradiotherapy (CRT) resistance in CRC¹⁶. Specifically, STAT3 enhances the tolerance of cancer cells to CRT treatments through mechanisms such as upregulating the expression of anti-apoptotic genes, promoting DNA repair and regulating the tumor microenvironment. Therefore, targeted inhibition of STAT3 has been recognized as a crucial strategy to reduce CRT treatment tolerance in cancer cells and improve therapeutic efficacy, highlighting its significant research value and clinical potential.

Recent studies have identified a number of ZNFs that regulate STAT3 activity. For instance, ZNF341 binds to the promoter of STAT3 and activates its transcriptional, thereby influencing immunity¹⁷. By contrast, ectopic expression of ZNF382 significantly reduces the STAT3 transcriptional activity at the promoters of its target oncogenes¹⁸. Additionally, TNF receptor associated factor 6 negatively regulates the Janus kinase (JAK)-STAT3 pathway by binding to and mediating the ubiquitylation of pathway components¹⁹. These findings underscore the notable role of ZNFs in STAT3 regulation, providing new research perspectives and potential targets for the development of targeted therapies.

The present study aimed to examine the expression level of ZNF263 in CRC tissues. In addition to this primary objective, the present study aimed to evaluate the impact of ZNF263 on various cellular aspects, including the proliferation, invasion, migration and EMT of CRC cells and its possible mechanisms. Furthermore, the present study aimed to confirm the effect of ZNF263 on CRT in patients with CRC. Through these comprehensive analyses, this study provided valuable insights into the multifaceted role of ZNF263 in CRC treatment.

Materials and methods

Cell lines and clinical specimens

The CRC cell lines, SW480 and HCT116, were purchased from Wuhan Punosai Life Sciences Co., Ltd. (Wuhan Pricella Biotechnology Co., Ltd.). Rigorous short tandem repeat analyses were conducted to authenticate these cell lines, followed by comprehensive tests to confirm the absence of mycoplasma contamination. The CRC cell lines were cultivated in Roswell Park Memorial Institute 1640 medium (Gibco; Thermo Fisher Scientific, Inc.) supplemented with 10% fetal bovine serum (FBS; Gibco; Thermo Fisher Scientific, Inc.) at 37 °C in a humidified chamber with a 5% CO₂ atmosphere.

From October, 2022 to January, 2024, 53 CRC samples and corresponding paracancerous tissues were collected at Gansu Provincial People's Hospital (Gansu, China). Before the collection process, informed consent was obtained from each patient. The present study received ethical approval from the Ethics Committee of Gansu Provincial Hospital (approval no. 2024–300), and all experiments were conducted in accordance with relevant guidelines and regulations.

Analysis of public data sets

A comprehensive understanding of ZNF263 expression was gained through extensive analysis of RNA levels. This analysis was conducted utilizing The Cancer Genome Atlas (TCGA) database. Changes in ZNF263 expression during CRC development were further explored by carefully evaluating tumor grade, lymph node metastasis and distant metastasis. The correlation between STAT3 and ZNF263 was confirmed by the online database, TIMER2.0 (<http://timer.cistrome.org/>), which provided a solid theoretical basis for the subsequent experimental design. In addition, the binding of ZNF263 to the STAT3 promoter sequence was further predicted using the UCSC Genome Browser (<http://timer.cistrome.org/>) and JaspAr (<https://jaspar.elixir.no/>) databases.

Immunohistochemistry (IHC) assay

The streptavidin-peroxidase method was employed to assess the expression of ZNF263 in CRC tissues and adjacent paracancerous tissues. Initially, the pathological paraffin sections were deparaffinized using xylene, followed by dehydration with an ethanol gradient. The sections were subjected to antigen retrieval by immersion in 10 mmol/l citrate buffer for 2 min, then 3% hydrogen peroxide was applied to inhibit endogenous peroxidases. The ZNF263 primary antibody (rabbit; 1:400; cat. no. PA5-57150; Invitrogen; Thermo Fisher Scientific, Inc.) was applied to the sections overnight at 4 °C. Next, the sections were incubated with HRP-labeled secondary antibody (Goat Anti-Rabbit IgG H&L; 1:1000; cat. no. ab205718; Abcam) for 2 h at 37 °C. After staining with 3,3'-diaminobenzidine, the sections were counterstained with hematoxylin and microscopic observation and scoring were conducted.

Scoring of the immunostaining was based on the degree of staining intensity and the percentage of positive cells. The percentage of positive cells was graded as 0 for no staining, 1 for < 30%, 2 for 30–60% and 3 for > 60%. Scoring of the staining intensity was conducted using a scale of 0 for no staining, 1 for light brown, 2 for brown and 3 for dark brown. In total, two experienced pathologists evaluated the study outcomes using a double-blinded quantitative method. The final score was obtained by multiplying the percentage and staining intensity scores. A score of ≥ 3 indicated a positive result, while a score < 3 indicated a negative result.

Construction of lentivirus and stable cell lines

Vectors carrying short hairpin (sh)RNA sequences were constructed utilizing the pHLV-U6-MCS-CMV-ZsGreen-PGK-PURO vector. The following vectors were used in the present study: shZNF263, shSTAT3 and shControl. A non-targeting shRNA control sequence was included in shControl. The shRNA sequences used in the present study are included in Table SI. Additionally, the ZNF263 and STAT3 gene sequences were inserted into pHLV-U6-MCS-CMV-ZsGreen-PGK-PURO to create lentiviral overexpression vectors. The resulting vectors were named oeZNF263 and oeSTAT3, respectively. The empty vector (Control) was used as the negative control.

Lentiviral packaging was performed using the triple plasmid lentiviral system. Briefly, plasmids (psPAX2, pMD2G and plasmids carrying target genes or shRNAs) were co-transfected into 293T cells using the Lipofiter Plasmid Transfection Reagent (Hanbio Biotechnology Co., Ltd). The solution containing virus particles was obtained 48 and 72 h post-transfection. The viral stock was concentrated and purified through ultracentrifugation (4 °C, 82,700 × g, 120 min), resulting in a high-titer lentiviral stock. Polybrene was used to transduce viruses into SW480 and HCT116 cells at 37 °C for 24 h, with a multiplicity of infection of 30–50. Following this, the virus medium was replaced with fresh medium. Puromycin (1.5 g/ml) was used to screen stably transfected cells. Finally, successful transfection was confirmed by western blotting.

RNA extraction and reverse-transcription quantitative polymerase chain reaction (RT-qPCR)

The TRIzol reagent (Invitrogen; Thermo Fisher Scientific, Inc.) was used to extract total RNA from CRC tissues or cells according to the manufacturer's instructions. RT reactions were conducted using the M5 Sprint qPCR RT kit with gDNA remover (Mei5 Biotechnology Co., Ltd,) in a 20 µl reaction volume, with the following conditions: 42 °C for 2 min, 50 °C for 5 min and 85 °C for 5 s. qPCR was performed using the 7500 real-time fluorescence quantitative PCR instrument system (Thermo Fisher Scientific, Inc.) and 2X M5 HiPer SYBR Premix EsTaq (Mei5 Biotechnology Co., Ltd.). The qPCR conditions consisted of an initial denaturation at 94 °C for 5 min, followed by 35 cycles at 94 °C for 40 s, 60 °C for 30 s and 72 °C for 60 s and a final extension at 72 °C for 7 min. The relative ZNF263 and STAT3 level was calculated using the $2^{-\Delta\Delta Cq}$ method. For cell lines, the following equations were used: $\Delta Cq = Cq_{\text{target}} - Cq_{\text{GAPDH}}$ and $\Delta\Delta Cq = \Delta Cq_{\text{expression vector}} - \Delta Cq_{\text{control vector}}$. The expression levels were standardized with respect to the control cells, which was set to 1.0. For clinical tissue samples, the $2^{-\Delta\Delta Cq}$ method was similarly used to determine the fold change in target gene expression levels using the following formula: $\Delta Cq = Cq_{\text{target}} - Cq_{\text{GAPDH}}$ and $\Delta\Delta Cq = \Delta Cq_{\text{tumor}} - \Delta Cq_{\text{non-tumor}}$. The expression levels were adjusted to healthy colorectal tissue, which was set to 1.0. The primer sequences used in the qPCR are shown in Table SII.

Chromatin immunoprecipitation (ChIP)

The Chromatin Immunoprecipitation Kit (JKR23002A; Genecreate) was used to conduct ChIP analysis. Briefly, 1×10^7 cells were cross-linked with 1% formaldehyde for 10 min at 37 °C, then quenched with glycine. The DNA was then fragmented using ultrasound. Following fragmentation, 5–10 µg DNA was incubated overnight at 4 °C with 5 µg ZNF263 primary antibody (mouse; cat. no. sc-135612; Santa Cruz Biotechnology, Inc.) and normal rabbit IgG (from the Chromatin Immunoprecipitation Kit). The precipitated DNA was then purified using resuspended magnetic beads. The corresponding promoter binding sites were amplified using PCR and the respective primer sequences shown in Table SII. For this, a PCR system (Takara Bio, Inc.), RT-PCR and Taq DNA polymerase (cat. no. EP0405; Thermo Fisher Scientific, Inc.) were utilized. The PCR thermocycler conditions were as follows: Initial denaturation for 5 min at 94 °C, 35 cycles at 94 °C for 40 s and 60 °C for 30 s and an extension step at 72 °C for 7 min.

Transient transfection and luciferase assay

The ZNF263 expression plasmid was obtained by cloning ZNF263 into the pCMVtag2A vector (Agilent Technologies, Inc.). SW480 or HCT116 cells were cultured in 24-well plates at a density of 1×10^5 cells/well. After 12–24 h of incubation, expression plasmid (0.6 µg; pCMV-ZNF263 or pCMV control), reporter plasmid (0.18 µg) (Promega Corporation) and PRL-TK plasmid (0.02 µg) (Promega Corporation) were co-transfected into the cells using Lipofectamine 3000 reagent. After 5 h of transfection, the cells were washed and placed in fresh medium containing 1% FBS and cultured for 48 h to recover. The cells were then subjected to a serum starvation assay. The luciferase activity was evaluated utilizing a dual luciferase assay kit (Promega Corporation), following the manufacturer's instructions. Lysis of the transfected cells was performed in Eppendorf microcentrifuge tubes, then the samples were centrifuged at 72,000 × g for 120 min at 4 °C. The luciferase activity was measured using a Modulus™ TD20/20 photometer (Turner Designs), with renin luciferase activity used for normalization.

Western blotting

The cells or tissues in each group were washed with pre-cooled PBS then incubated with lysis buffer (Beijing Solarbio Science & Technology Co., Ltd) at 4 °C for 30 min. The resulting supernatant was collected through centrifugation (15 min, 4 °C, 12,000 × g). Next, 30 µg of protein from each group were separated using 10% SDS-PAGE (cat. no. P2012; NCM Biotech), then transferred onto PVDF membranes (cat. no. IPVH00010; Merck KGaA). The membranes were blocked and then incubated with the following primary antibodies overnight at 4 °C: ZNF263 (mouse; 1:500; cat. no. sc-135612; Santa Cruz Biotechnology, Inc.), STAT3 (rabbit; 1:1,000; cat. no. ab109085; Abcam), N-cadherin (rabbit; 1:1,000; cat. no. WL01047; Wanleibio Co., Ltd.), E-cadherin (rabbit; 1:1,000; cat. no. WL01482; Wanleibio Co., Ltd.), Snail (rabbit; 1:1,000; cat. no. WL01863; Wanleibio Co., Ltd.), Vimentin (rabbit; 1:1,000; cat. no. WL01960; Wanleibio Co., Ltd.) and GAPDH (rabbit; 1:5,000; cat. no. ab245355; Abcam). After primary antibody incubation, the membranes were treated with the corresponding secondary

antibodies (antirabbit, HRPconjugated;1:2,000; ab150077; Abcam) (antimouse, HRPconjugated;1:2,000; ab150113; Abcam) for 1 h. Finally, protein bands were visualized using chemiluminescent reagents.

EdU cell proliferation assay

Cells (2×10^5) were seeded into a 6-well plate and, once the cells had fully adhered, EdU working solution (Dalian Meilun Biology Technology Co., Ltd.) was added. The cells were then incubated for 2 h. Following the manufacturer's instructions, the EdU-555 Cell Proliferation Assay Kit (Dalian Meilun Biology Technology Co., Ltd.) was used to stain the cells. The EdU-labeled cells were then visualized using a fluorescence microscope.

Cell counting Kit-8 (CCK8) assay

Cells (2×10^3) were seeded into 96-well plates and CCK-8 (Weiboxin Biotechnology Co., Ltd.) was used to evaluate cell proliferation on days 1, 2, 3, 4 and 5.

Colony formation assay

Cells (1×10^3) were seeded into 6-well plates and cultured for 2 weeks. The resulting colonies were then incubated with 4% paraformaldehyde (Wuhan Pmk Biotechnology Co., Ltd.) at 25 °C for 20 min, to ensure the cellular structure remained intact. Next, the colonies were stained with 0.1% crystal violet (Beijing Solarbio Science & Technology Co., Ltd.) at 25 °C for 5 min. Only colonies with > 50 cells were considered for further examination.

Transwell invasion and migration assays

The cells were first seeded into the top chamber of Transwell inserts (Corning, Inc.). To conduct the invasion assay, 50 μ l Matrigel was added to the top chamber. The ability of the cells to migrate and invade was measured by calculating the number of cells that migrated or invaded into the bottom chamber of the Transwell plate. The cells were seeded in serum-free medium in the upper chamber, while medium supplemented with 20% FBS was added to the lower chamber to incite chemotaxis. The Transwell plates were then placed in a 5% CO₂ incubator at 37 °C for 48 h. After incubation, the cells were fixed with 4% paraformaldehyde (Wuhan Pmk Biotechnology Co., Ltd.), then stained with 0.2% crystal violet (Beijing Solarbio Science & Technology Co., Ltd.) for visualization and imaging.

Cell radiotherapy

Cells were seeded into either 96- or 6-well plates and then placed in a humidified incubator for 24 h to acclimatize to the culture conditions. Following this acclimatization period, the cells were irradiated at the specified doses according to the experimental design. For cells in the 96-well plates, CCK-8 reagent (Weiboxin Biotechnology Co., Ltd.) was added on days 1, 2, 3, 4 and 5 after irradiation to assess the proliferation. For cells in the 6-well plates, incubation was continued until colony formation occurred. After the colonies were fixed, crystal violet (Beijing Solarbio Science & Technology Co., Ltd.) staining was performed and the number of colonies in each group was counted. Unirradiated cells were included as a control group to facilitate the comparison of the survival and proliferation rates among the experimental groups.

Cisplatin treatment

Cells were seeded into 96- or 6-well plates and incubated for at least 12 h. In the 96-well plates, different concentrations of cisplatin (APeXBIO Technology LLC) were added to the cells, followed by an additional 48-h incubation. CCK-8 was then added to the cells and the optical density (OD) was determined. The cell viability was calculated using the formula: (OD of treated cells/OD of vehicle-treated cells) \times 100%. The cells in the 6-well plates were treated with different concentrations of cisplatin and incubated until colonies formed. After the colonies were fixed, crystal violet (Beijing Solarbio Science & Technology Co., Ltd.) staining was performed and the number of colonies in each group was counted. The effect of cisplatin on cell proliferation and colony formation was evaluated using cells treated with the vehicle, which does not contain cisplatin but is treated under the same conditions as the drug treatment group, as a control.

Statistical analysis

The experiments were conducted independently and repeated at least three times. Statistical analysis was performed using SPSS software (version 25; IBM Corp.), and the outcomes are presented as the mean \pm SD. Categorical data were evaluated using the χ^2 test. Comparisons between groups were performed using Student's t-test (paired t-test for paired data, independent samples t-test for unpaired data) or one-way ANOVA followed by Tukey's or Dunnett's post hoc tests. Graphical analysis was conducted using GraphPad Prism 9.5.1 software (Dotmatics). $P < 0.05$ was considered to indicate a statistically significant difference.

Results

ZNF263 is upregulated in CRC tissues

After analyzing data from TCGA database, it was observed that the ZNF263 expression level was significantly higher in CRC tissues compared with normal tissues (Fig. 1A and S1A). To further explore this finding, the clinical significance of ZNF263 in CRC tissues was analyzed through IHC. The results showed that ZNF263 was highly expressed in CRC tissues, and this upregulation was associated with various factors such as tumor grade, lymph node metastasis, vascular metastasis and nerve invasion (Fig. 1B and S2A; Table 1). Building on these findings, the expression of ZNF263 in eight sets of CRC and adjacent non-tumor tissues was examined via western blotting and RT-qPCR. The results showed that ZNF263 was notably elevated in CRC tissues compared with the adjacent normal tissues (Fig. 1C, S3A and 1D).

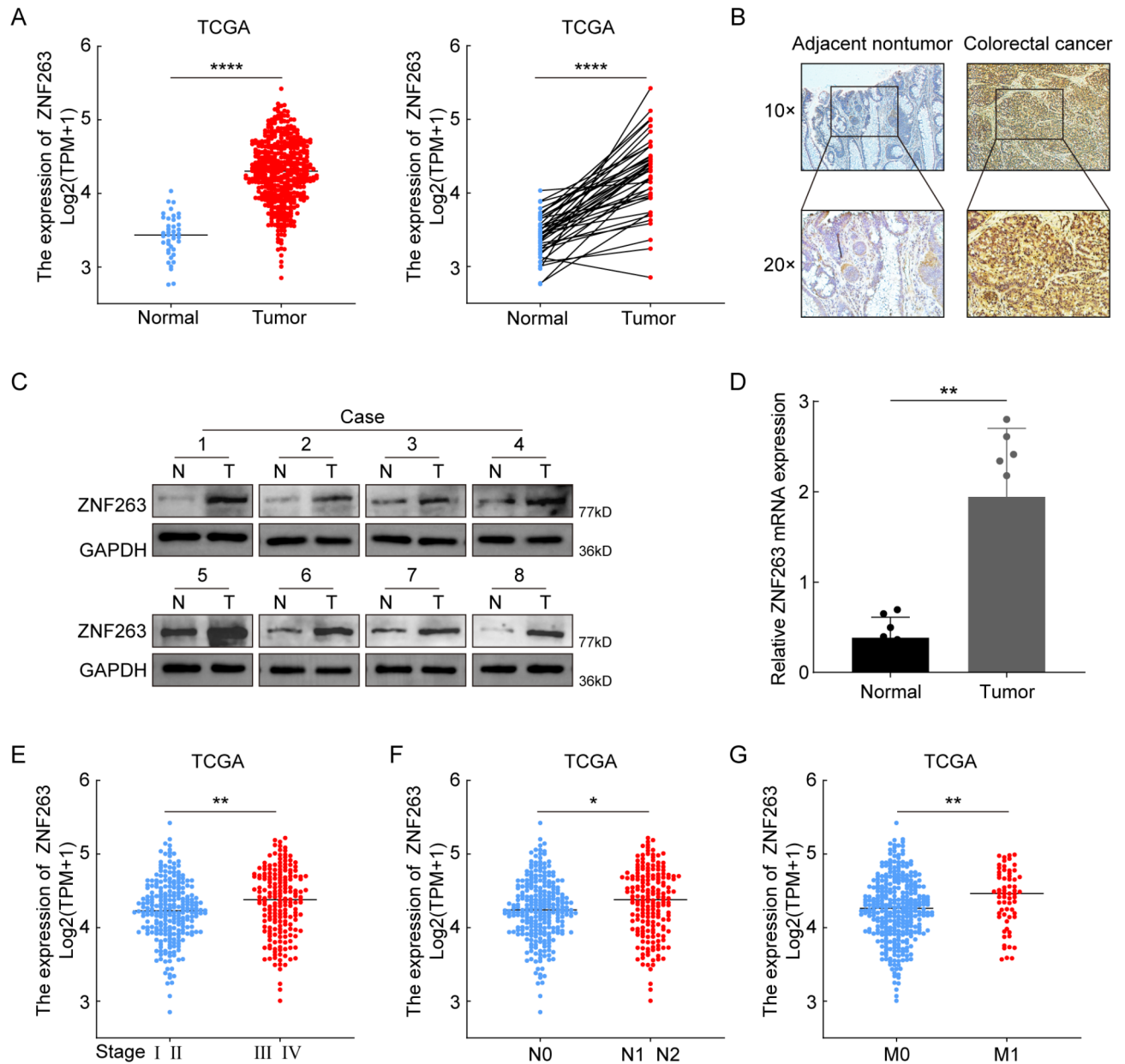


Fig. 1. ZNF263 is upregulated in CRC tissues. (A) The expression levels of ZNF263 in CRC and adjacent non-tumor tissues (data from TCGA). (B) Representative images displaying ZNF263-targeted staining in CRC tissues alongside paired non-tumor tissues. (C) The relative protein expression levels of ZNF263 in eight pairs of CRC and corresponding adjacent tissues were determined by western blotting analysis (ZNF263, 77 kDa; GAPDH, 36 kDa). (D) The relative mRNA expression levels of ZNF263 in eight pairs of CRC and corresponding adjacent tissues were determined by reverse transcription-quantitative polymerase chain reaction. Analysis revealed the association between ZNF263 expression and (E) tumor grading, (F) lymph node metastasis and (G) distant metastasis in CRC (data from TCGA). Experiments were repeated at least three times and data are presented as the mean \pm SD. * P < 0.05, ** P < 0.01, **** P < 0.0001. ZNF263, zinc finger protein 263; CRC, colorectal cancer; TCGA, The Cancer Genome Atlas.

Moreover, the expression of ZNF263 in individual patient groups in TCGA dataset was characterized based on clinical characteristics (Table 2). There was a significant association between tumor grade and ZNF263 expression (Fig. 1E). In addition, patients with lymph node metastasis and distant metastasis showed increased levels of ZNF263 expression (Fig. 1F and G). These findings collectively suggest an increase in ZNF263 expression occurs in CRC, indicating a possible role in the progression and metastasis of CRC.

ZNF263 significantly promotes the proliferation, invasion and migration of CRC cells

Next, the expression level of ZNF263 in CRC cell lines was analyzed (Fig. S4A). SW480 and HCT116 represented ZNF263 low-expressing and high-expressing cells, respectively. To ensure a comprehensive analysis, these two

Clinicopathological variables	Number (n = 53)	ZNF263 expression		P-value
		High (n = 30)	Low (n = 23)	
Age, years				0.569
≤ 55	23	12	11	
> 55	30	18	12	
Gender				0.637
Male	28	15	13	
Female	25	15	10	
Tumor size (cm)				0.132
≤ 5	27	18	9	
> 5	26	12	14	
AJCC stage				< 0.01**
I and II	19	6	13	
III and IV	34	24	10	
T stage				0.289
T1 and T2	18	12	6	
T3 and T4	35	18	17	
N stage				0.028*
N0	21	8	13	
N1-N3	32	22	10	
Vascular metastasis				< 0.01**
Yes	23	18	5	
No	30	12	18	
Lymphatic invasion				0.875
Yes	27	15	12	
No	26	15	11	
Neurological violation				0.03†
Yes	34	23	11	
No	19	7	12	

Table 1. Associations between ZNF263 expression and clinicopathological parameters in 53 patients with colorectal cancer. AJCC American Joint Committee on Cancer. ** $P < 0.01$, * $P < 0.05$.

cell lines were selected to further investigate the effect of ZNF263 on CRC progression. For this purpose, two stable cell lines were established (Fig. 2A, S3B and S3C). The results of the CCK-8 and EdU assays showed that ZNF263 overexpression promoted cell proliferation (Fig. 2B and C), which was consistent with the results of the colony formation assays (Fig. 2D). Conversely, the proliferation and colony formation abilities of CRC cells were inhibited upon knockdown of ZNF263 (Fig. 2B-D). In addition, the overexpression of ZNF263 promoted the invasion and migration of SW480 cells, while the knockdown of ZNF263 decreased the invasion and migration of HCT116 cells (Fig. 2E and F). Supporting these observations, cells overexpressing ZNF263 exhibited reduced E-cadherin protein expression and increased N-cadherin, vimentin and Snail protein expression. However, ZNF263 knockdown increased the protein expression of E-cadherin and decreased the protein expression of N-cadherin, vimentin and Snail (Fig. 2G, S3D and S3E). Collectively, these experimental results indicate that ZNF263 may act as an oncogene to promote the proliferation, invasion, migration and EMT of CRC cells, suggesting that upregulation of ZNF263 may contribute to the aggressive phenotype of CRC.

STAT3 is a target of ZNF263

STAT3 is a signaling protein that mediates various cellular processes^{20,21}. Given its pivotal role, it was next determined whether ZNF263 affects the transcriptional activation of STAT3 to promote CRC progression. First, the GEPIA and TCGA databases were used to confirm a significant correlation between STAT3 and ZNF263 expression (Fig. 3A, S1B and S1C). Subsequently, the mRNA and protein levels of STAT3 were then examined in cells with ZNF263 overexpression or knockdown. The results showed that overexpression of ZNF263 increased the STAT3 mRNA and protein levels, whereas downregulation of ZNF263 decreased the STAT3 mRNA and protein levels (Fig. 3B and C, S3F and S3G).

It has been demonstrated that ZNFs can directly bind to STAT3 to regulate its transcriptional activity¹⁷⁻¹⁹. Building on this knowledge, the UCSC Genome Browser database was utilized to demonstrate the binding of ZNF263 to the STAT3 promoter region (Fig. 3D). Further analysis using the JASPAR database was conducted to obtain the binding site of the ZNF263 zinc finger structural domain (Fig. 3E). To confirm this interaction, direct binding of ZNF263 to the STAT3 promoter region was further demonstrated by ChIP analysis (Fig. 3F). To validate the functional impact of this interaction, constructs expressing the STAT3 promoter and pCMV-ZNF263 were co-transfected into cells and the luciferase activity was assessed. The findings revealed a significant

Clinicopathological variables	Number (<i>n</i> = 644)	ZNF263 expression		<i>P</i> -value
		Low (322)	High (322)	
Age, years				0.111
≤ 65	276	368	148	
> 65	368	194	174	
Gender				0.813
Male	343	173	170	
Female	301	149	152	
AJCC stage				0.029*
I and II	349	190	159	
III and IV	274	125	149	
T stage				0.970
T1 and T2	131	65	66	
T3 and T4	510	254	256	
N stage				0.025*
N0	368	198	170	
N1 and N2	272	122	150	
M stage				0.009**
M0	475	248	227	
M1	89	33	56	
Lymphatic invasion				0.787
Yes	232	116	116	
No	350	179	171	
Perineural invasion				0.440
Yes	60	25	35	
No	175	83		

Table 2. Relationship between ZNF263 expression and clinicopathologic parameters in 644 colorectal cancer patients in the TCGA database. AJCC American Joint Committee on Cancer. ***P* < 0.01, **P* < 0.05.

increase in luciferase activity in cells transfected with the STAT3 promoter (Fig. 3G). These outcomes indicate that ZNF263 binds directly to certain sites on the STAT3 promoter, leading to the transcriptional activation of subsequent gene expression.

ZNF263 promotes CRC cell proliferation and migration by upregulating STAT3

To investigate the effects of the ZNF263-STAT3 axis on CRC cell biology, rescue experiments were conducted. First, the STAT3 knockdown model was constructed in the SW480 cell line that stably overexpressed ZNF263; then, the STAT3 overexpression model was constructed in the HCT116 cell line that stably knocked down ZNF263. Subsequently, the changes in the protein expression levels of STAT3 after overexpression or knockdown were detected and verified by Western blotting (Fig. 4A, S3H and S3I). Subsequent functional assays, including CCK-8, EdU and colony formation rescue assays, demonstrated that STAT3 knockdown significantly inhibited the proliferative ability of SW480 cells. Conversely, STAT3 overexpression significantly restored the proliferative ability of HCT116 cells (Fig. 4B-D). Furthermore, Transwell and Western blotting assays revealed that STAT3 knockdown significantly inhibited the invasion, migration and EMT abilities of SW480 cells, while STAT3 overexpression significantly restored these abilities in HCT116 cells (Fig. 4E-G, S3J and S3K). These findings collectively suggest that ZNF263 promotes the malignant behavior of CRC by binding and activating STAT3.

ZNF263 increases the resistance of CRC cells to CRT

At present, in addition to surgery, the two main conventional treatments for CRC are chemotherapy and radiotherapy. However, the development of therapeutic resistance imposes a limitation on the effectiveness of these treatments. To gain an insight into this issue, a series of comparative experiments were conducted to analyze the effects of ZNF263 on the viability and colony formation ability of cells under different doses of radiation and cisplatin treatments. The results indicated that the viability and colony formation capacity of SW480 cells when exposed to irradiation (Fig. 5A and B) or cisplatin (Fig. 5C and D) treatments, were significantly increased due to overexpression of ZNF263. These findings collectively demonstrate the critical regulatory function of ZNF263 in the chemoresistance of CRC cells.

Discussion

In the present study it was demonstrated that ZNF263 expression was significantly increased in CRC, which was verified using data from TCGA database and collected CRC samples. Furthermore, it was shown that high expression of ZNF263, a transcription factor, was closely associated with tumor grade, lymph node metastasis and distant metastasis in patients with CRC. The overexpression of ZNF263 was also found to promote the

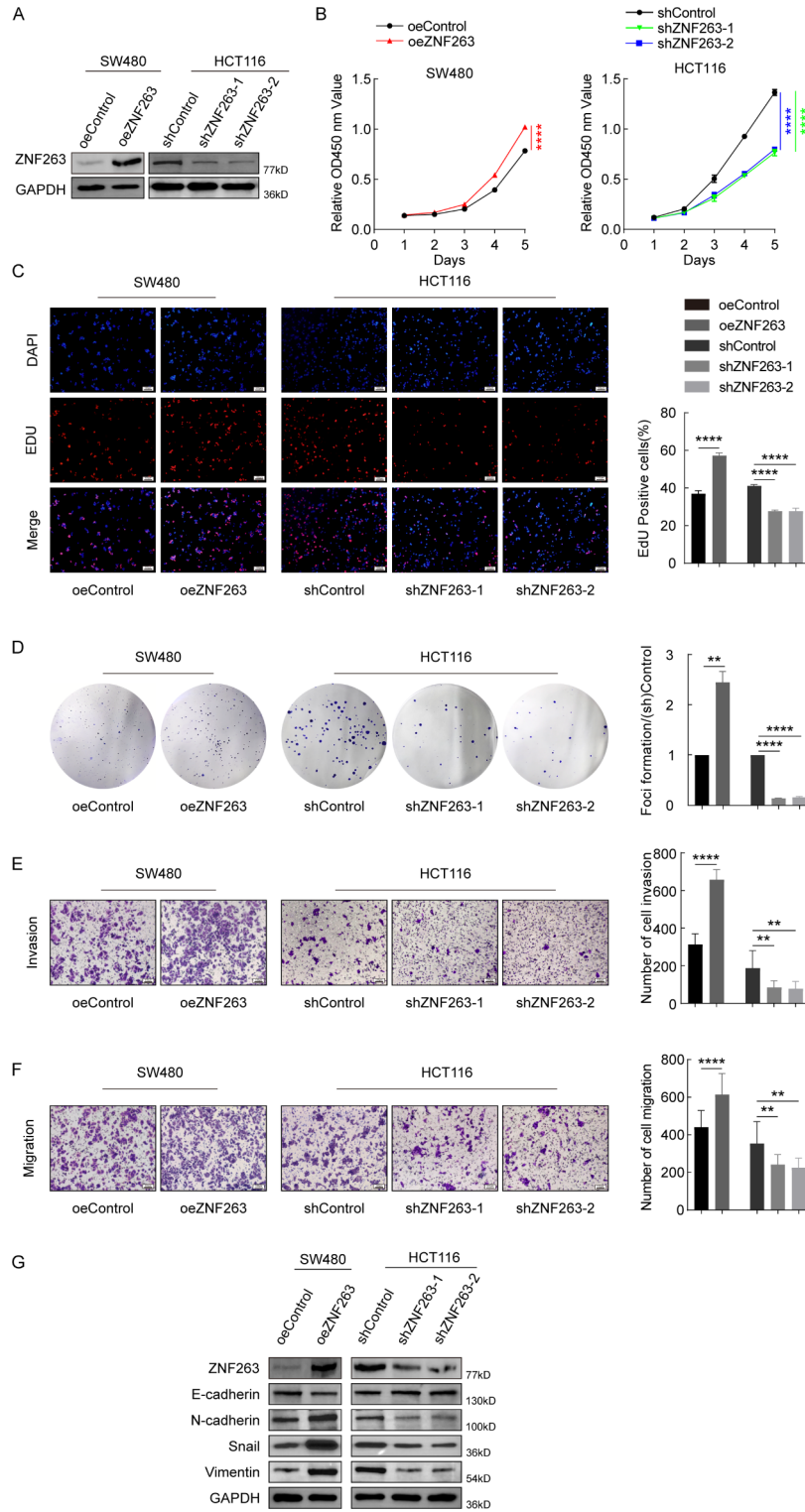


Fig. 2. ZNF263 significantly promotes the proliferation, invasion and migration of colorectal cancer cells. **(A)** ZNF263 protein expression in SW480 and HCT116 cells. The proliferation of SW480 and HCT116 cells was assessed using **(B)** Cell Counting Kit-8, **(C)** EdU and **(D)** colony formation assays. The **(E)** invasion and **(F)** migration abilities of SW480 and HCT116 cells were evaluated using Transwell assays. **(G)** The protein expression level of E-cadherin, N-cadherin, Snail, Vimentin and Snail in SW480 and HCT116 cells was determined by western blotting. Experiments were repeated at least three times and data are presented as the mean \pm SD. $**P < 0.01$, $****P < 0.0001$. ZNF263, zinc finger protein 263.

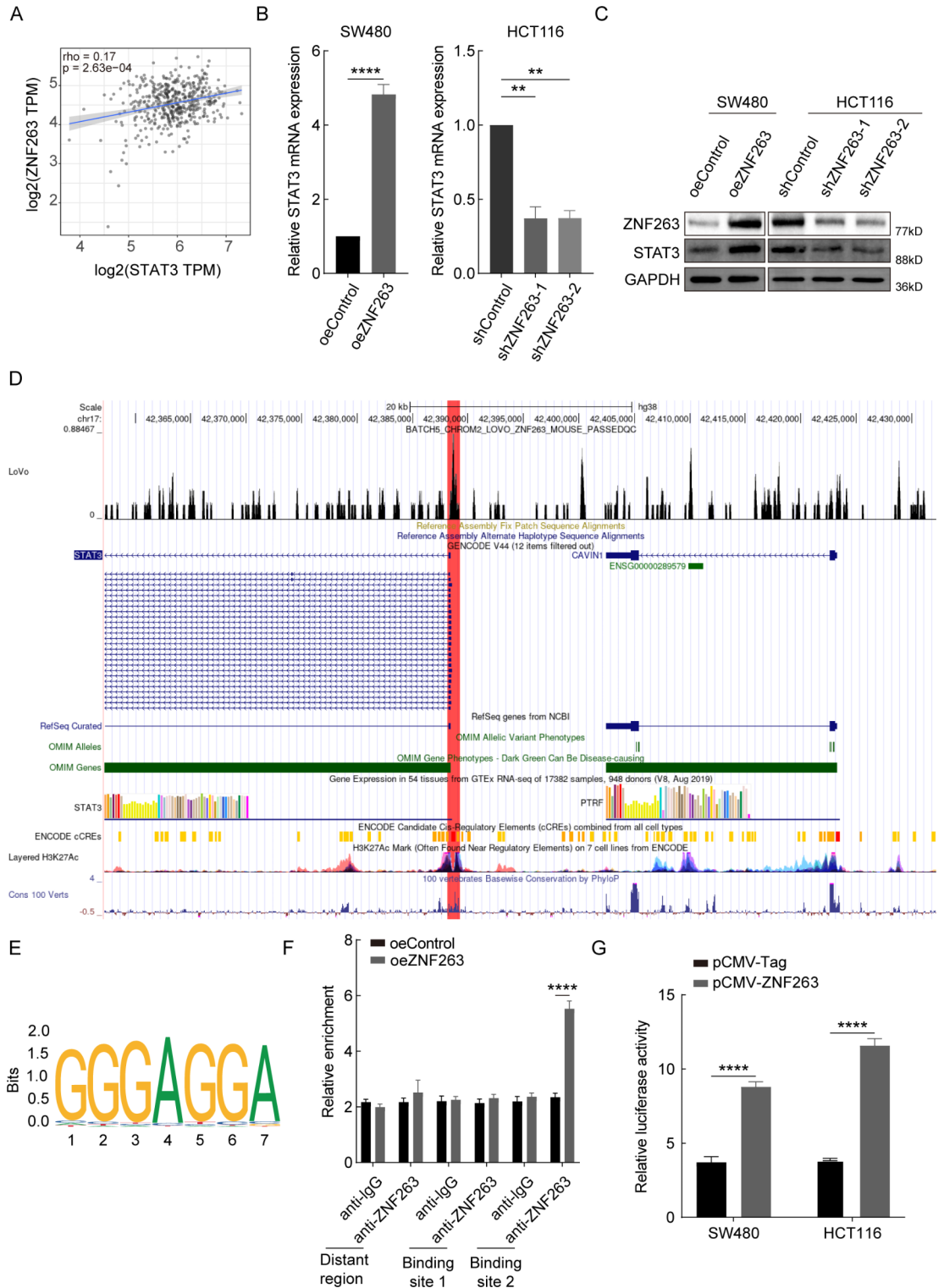


Fig. 3. STAT3 is a target of ZNF263. (A) TIMER2.0 (<http://timer.cistrome.org/>) was used to analyze the correlation between ZNF263 and STAT3. Detection of STAT3 (B) mRNA and (C) protein expression. (D) The UCSC Genome Browser database (<http://timer.cistrome.org/>) was used to predict that ZNF263 binds to the promoter of STAT3. (E) The JASPAR database (<https://jaspar.elixir.no/>) was used to predict the binding site of the ZNF263 zinc finger structural domain. (F) The binding of ZNF263 to the STAT3 promoter region in CRC cells was verified by chromatin immunoprecipitation. (G) Luciferase activity driven by the STAT3 promoter was evaluated in CRC cells. Experiments were repeated at least three times and data are presented as the mean \pm SD. ** $P < 0.01$, **** $P < 0.0001$. ZNF263, zinc finger protein 263; CRC, colorectal cancer; STAT3, signal transducer and activator of transcription 3.

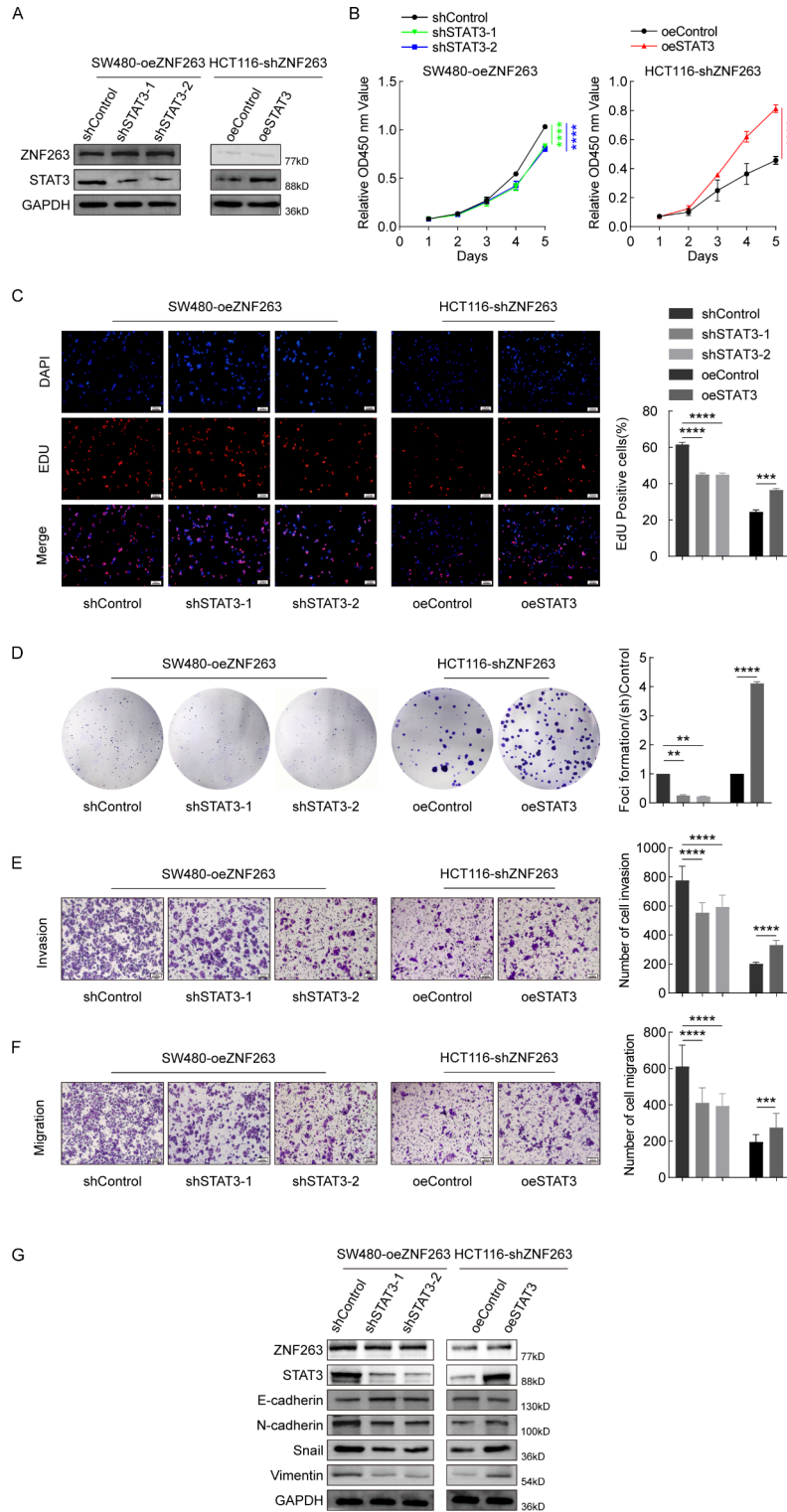


Fig. 4. ZNF263 promotes CRC cell proliferation and migration by upregulating STAT3. **(A)** The expression of STAT3 protein in SW480 and HCT116 cells. The proliferation of SW480 and HCT116 cells was assessed using **(B)** Cell Counting Kit-8, **(C)** EdU and **(D)** colony formation assays. The **(E)** invasion and **(F)** migration abilities of SW480 and HCT116 cells was analyzed using Transwell assays. **(G)** Western blotting was used to analyze the effect of STAT3 on the protein expression level of E-cadherin, N-cadherin, Vimentin and Snail in SW480 and HCT116 cells. Experiments were repeated at least three times and data are presented as the mean \pm SD. $**P < 0.01$, $***P < 0.001$, $****P < 0.0001$. ZNF263, zinc finger protein 263; STAT3, signal transducer and activator of transcription 3.

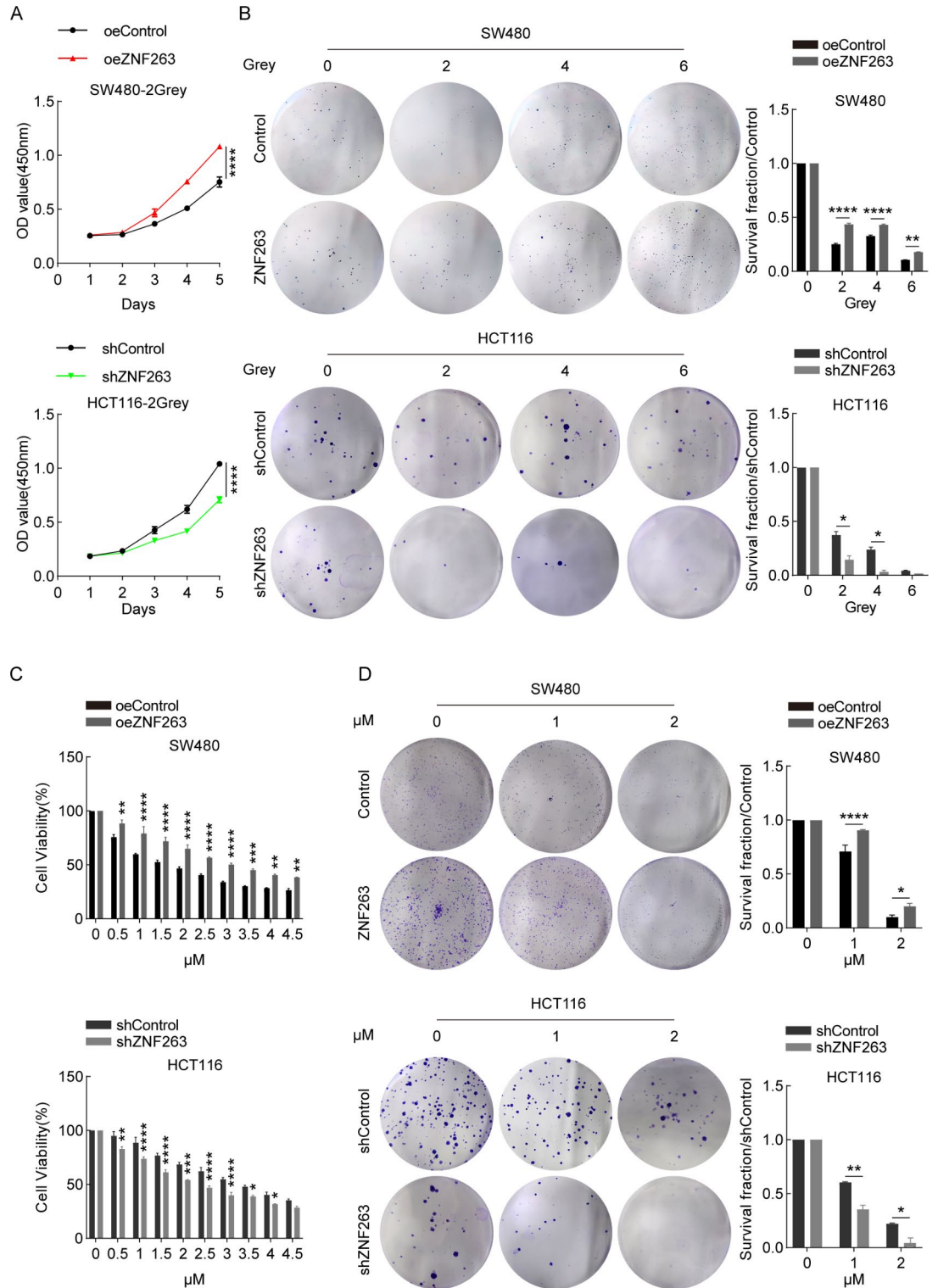


Fig. 5. ZNF263 increases the resistance of colorectal cancer cells to chemoradiotherapy. **(A)** The proliferative capacity of irradiated SW480 and HCT116 cells was assessed using the CCK-8 assay. **(B)** Representative images and quantification of the colony formation of SW480 and HCT116 cells exposed to varying doses of X-ray radiation. **(C)** The survival of SW480 and HCT116 cells treated with different concentrations of cisplatin was evaluated using the CCK-8 assay. **(D)** Representative images and quantification of the colony formation of SW480 and HCT116 cells treated with varying doses of cisplatin. Experiments were repeated at least three times and data are presented as the mean \pm SD. * $P < 0.05$, ** $P < 0.01$, **** $P < 0.0001$. ZNF263, zinc finger protein 263; CCK-8, Cell Counting Kit-8.

proliferation, invasion, migration and EMT of CRC cells, while increasing STAT3 expression and mRNA stability. By contrast, knockdown of ZNF263 inhibited the malignant behavior of CRC cells and decreased STAT3 expression and mRNA stability. Moreover, the effects of ZNF263 on CRC cells could be significantly reversed by overexpressing or knocking down STAT3. Further experiments in the present study showed that ZNF263 also promoted the resistance of CRC cells to CRT. The aforementioned results were validated through the use of TCGA database and CRC samples collected in the present study, combined with *in vitro* cellular experiments and molecular biology techniques to ensure the reliability and validity of the findings. The high expression of ZNF263 in CRC observed in the present study and its regulatory effect on STAT3 enhances the understanding of the mechanisms underlying CRC development. These results align with certain previous studies and also suggest new research directions^{9,10}, such as further exploration of the molecular mechanism underpinning the interaction between ZNF263 and STAT3, as well as the potential of ZNF263 as a therapeutic target for CRC.

ZNF263 has been identified as an oncogene in various cancer types and is critical in promoting malignant biological processes, including cell proliferation, apoptosis resistance, migration and invasion^{9,10,22}. A previous study has demonstrated that ZNF263 regulates the circular FOXP1 RNA/miRNA-423-5p/U2 small nuclear RNA auxiliary factor 2 axis, promoting the proliferation, migration and invasion of renal cancer cell⁸. Moreover, it has been reported that ZNF263 activates RNF126 to promote proliferation and EMT in pancreatic cancer¹¹. Despite these findings, to the best of our knowledge, research has not yielded significant information regarding the role of ZNF263 in CRC. This study suggests that ZNF263 serves a pivotal role in the malignant progression of CRC. This is consistent with the known functions of ZNF263 in other cancer types, further underscoring its importance as an oncogene. However, unlike previous studies, the present study emphasized the specific impact of ZNF263 in CRC, suggesting a potential mechanism by which ZNF263 promotes the malignant progression of CRC by binding and activating STAT3.

STAT proteins have essential roles in cancer proliferation, invasion and migration^{23,24}. Among these proteins, the aberrant activation of STAT3 is particularly associated with these processes, making it a potential therapeutic target^{25,26}. One of the main factors contributing to the poor survival prognosis of patients with CRC is the increased expression of STAT3 in cancer cells. This elevated STAT3 expression level can also be utilized as a diagnostic tool for patients with cancer²⁷. It has also been confirmed that the occurrence and development of CRC are significantly linked to STAT3²⁸. Moreover, increased STAT3 expression levels have been associated with metastasis and drug resistance in patients with CRC^{16,29}, as well as with autophagy and apoptosis resistance^{13,30}. STAT3 also promotes CRC cell proliferation by stimulating glycolysis and facilitates metastasis by inducing EMT³¹. These findings underscore that STAT3 may have a crucial role in promoting cancer progression in CRC. However, the precise mechanisms underlying STAT3 dysregulation in CRC remain unclear. The present study addressed this gap by demonstrating that STAT3 is a binding target of ZNF263. Specifically, it was found that ZNF263 activates STAT3 expression by binding to its promoter region. In the present study, inhibition of STAT3 significantly suppressed ZNF263-mediated CRC proliferation, invasion, migration and EMT, whereas overexpression of STAT3 reversed the effects induced by downregulation of ZNF263. These results suggest that ZNF263 serves a pivotal role in CRC progression through the modulation of STAT3, highlighting the potential of targeting the ZNF263-STAT3 axis as a therapeutic strategy in CRC.

The use of platinum-based drugs in chemotherapy for patients with CRC is crucial, but its effectiveness is limited by resistance³². This resistance presents a significant obstacle to treatment. The initial treatment for patients with advanced or metastatic CRC is a combination therapy, which includes cisplatin, one of the most widely used antitumor drugs. However, the efficacy of cisplatin is also compromised by resistance. A previous study has demonstrated that ZNF263 increases the resistance of HCC to chemotherapy by activating the endoplasmic reticulum stress-related autophagy mechanism¹⁰. Additionally, ZNF263 has been shown to cooperate with ZNF31 to promote drug resistance in pancreatic cancer through trans-activation of RNF126¹¹. In the present study, it was confirmed that ZNF263 also promotes cisplatin resistance in CRC cells, consistent with the aforementioned findings. Specifically, the experimental results showed that CRC cells with elevated ZNF263 levels exhibited higher resistance to cisplatin treatment. These findings suggest that ZNF263 has a crucial role in mediating chemotherapy resistance across different cancer types, including CRC. However, the exact mechanism by which ZNF263 promotes cisplatin resistance in CRC remains unclear. Understanding the molecular pathways and key interactions involved in ZNF263-mediated resistance is crucial for developing targeted therapies to enhance chemotherapy sensitivity and improve treatment outcomes for CRC patients.

There are certain limitations to the present study that should be noted. First, a detailed explanation for how ZNF263 contributes to the resistance of CRC to CRT was not elucidated. Second, there are differences in the use of radiotherapy in clinical CRC treatment. In the treatment of rectal cancer, radiotherapy is usually used for preoperative neoadjuvant therapy to reduce tumor size and decrease the risk of postoperative recurrence; postoperative radiotherapy may also be used to manage incompletely resected lesions. However, for colon cancer, the use of radiotherapy is relatively rare and is mainly focused on the treatment of locally recurrent or metastatic cases. In addition, the present study did not include animal experimental validation. Including *in vivo* experiments would significantly strengthen the relevance of the findings of the present study and facilitate their translation into clinical applications. Although the results of the present study suggest that targeting ZNF263 could be a theoretical basis for treating patients with CRC who are resistant to CRT, this hypothesis remains to be tested in clinical settings. The lack of clinical data means that the direct applicability of the study findings to patient treatment remains uncertain. Addressing these limitations in future research will be crucial for enhancing the understanding of the role of ZNF263 in CRT resistance.

ZNF263 is a highly specific and multifunctional protein that can precisely regulate the expression of specific genes and other biological processes, making it a potential therapeutic target in cancer therapy¹⁰. Despite its potential, there are significant challenges in achieving specificity in drug design and ensuring effective delivery to the nucleus. One major challenge is the precise delivery of ZNF263-targeted drugs to the nucleus of cancer

cells. However, continuous technological advances offer promising solutions. For instance, the development of nanotechnology can improve the delivery efficiency and specificity of ZNF263-targeted therapies by encapsulating the drugs in nanoparticles that can specifically target cancer cells and release their payload within the nucleus^{33,34}. Furthermore, gene editing technologies, particularly those based on the CRISPR-Cas9 system, hold great promise for precisely regulating ZNF263 expression³⁵. This technology can be used to edit the genome at specific locations, potentially allowing for the targeted activation or suppression of ZNF263 in cancer cells, thereby improving therapeutic efficacy³⁶. As these technologies develop, the clinical application of ZNF263 as a targeted drug in personalized therapy becomes increasingly feasible. The potential mechanisms of ZNF263 in cancer treatment include inhibiting tumor cell proliferation and metastasis by regulating the STAT3 pathway and enhancing the sensitivity of cancer cells to CRT. These strategies provide new therapeutic options in the field of cancer treatment, which are expected to notably improve the prognosis and quality of life of patients with CRC.

In summary, the findings of the present study revealed that ZNF263 was highly expressed in CRC tissues and its overexpression promoted CRC cell progression through STAT3 activation. Conversely, downregulation of STAT3 significantly suppressed ZNF263-mediated CRC cell progression. Furthermore, ZNF263 enhanced CRC cell resistance to CRT. In conclusion, the present study identified a pivotal role of ZNF263 in CRC progression and resistance to treatment, suggesting that targeting ZNF263 could be a promising strategy for developing more effective therapeutics for CRC. Future research should focus on the mechanisms underlying the ZNF263 and STAT3 interaction and explore the potential clinical applications of ZNF263 inhibitors in CRC therapy.

Data availability

Data is available from corresponding authors upon reasonable request.

Received: 5 June 2024; Accepted: 9 September 2024

Published online: 18 September 2024

References

- Benson, A. B. *et al.* Colon Cancer, Version 2.2021, NCCN Clinical Practice Guidelines in Oncology. *J. Natl. Compr. Cancer Network: JNCCN* **2**(3), 329–359. <https://doi.org/10.6004/jnccn.2021.0012> (2021).
- Brandi, G. *et al.* Is post-transplant chemotherapy feasible in liver transplantation for colorectal cancer liver metastases? *Cancer Commun. (London, England)* **40**(9), 461–464. <https://doi.org/10.1002/cac2.12072> (2020).
- Dall'Olio, F. G. *et al.* Immortal time bias in the Association between Toxicity and Response for Immune Checkpoint Inhibitors: A meta-analysis. *Immunotherapy* **13**(3), 257–270. <https://doi.org/10.2217/imt-2020-0179> (2021).
- Rizzo, A. *et al.* Peripheral neuropathy and headache in cancer patients treated with immunotherapy and immuno-oncology combinations: The MOUSEION-02 study. *Expert Opin. Drug Metabolism Toxicol.* **17**(12), 1455–1466. <https://doi.org/10.1080/17425255.2021.2029405> (2021).
- Hong, K. *et al.* Comprehensive analysis of ZNF family genes in prognosis, immunity, and treatment of esophageal cancer. *BMC Cancer* **3**(1), 301. <https://doi.org/10.1186/s12885-023-10779-5> (2023).
- Yan, D. *et al.* Developing ZNF gene signatures predicting radiosensitivity of patients with breast cancer. *J. Oncol.* **2021**, 9255494. <https://doi.org/10.1155/2021/9255494> (2021).
- Wang, L. *et al.* Chromatin-associated OGT promotes the malignant progression of hepatocellular carcinoma by activating ZNF263. *Oncogene* **42**(30), 2329–2346. <https://doi.org/10.1038/s41388-023-02751-1> (2023).
- Fang, L., Ye, T., An, Y. & Circular, RNA FOXP1 induced by ZNF263 upregulates U2AF2 expression to accelerate renal cell carcinoma tumorigenesis and warburg effect through sponging Mir-423-5p. *J. Immunol. Res.* **2021**, 8050993. <https://doi.org/10.1155/2021/8050993> (2021).
- Yu, Z. *et al.* The EGFR-ZNF263 signaling axis silences SIX3 in glioblastoma epigenetically. *Oncogene* **39**(15), 3163–3178. <https://doi.org/10.1038/s41388-020-1206-7> (2020).
- Xu, J., Zhou, Y., Wang, Q., Liu, Y. & Tang, J. Zinc finger protein 263 upregulates interleukin 33 and suppresses autophagy to accelerate the malignant progression of non-small cell lung cancer. *Clin. Translational Oncology: Official Publication Federation Span. Oncol. Soc. Natl. Cancer Inst. Mexico* **26**(4), 924–935. <https://doi.org/10.1007/s12094-023-03325-z> (2024).
- Zhang, J. *et al.* ZNF263 cooperates with ZNF31 to promote the drug resistance and EMT of pancreatic cancer through transactivating RNF126. *J. Cell. Physiol.* **239**(6), e31259. <https://doi.org/10.1002/jcp.31259> (2024).
- Liu, X. *et al.* SNORA28 promotes proliferation and radioresistance in colorectal cancer cells through the STAT3 pathway by increasing H3K9 acetylation in the LIFR promoter. *Adv. Sci. (Weinheim, Baden-Wuerttemberg, Germany)* **26**, e2405332. <https://doi.org/10.1002/adv.202405332> (2024).
- Baniya, M. K., Kim, E. H. & Chun, K. S. Terfenadine, a histamine H1 receptor antagonist, induces apoptosis by suppressing STAT3 signaling in human colorectal cancer HCT116 cells. *Front. Pharmacol.* **15**, 1418266. <https://doi.org/10.3389/fphar.2024.1418266> (2024).
- Zhang, Z. H. *et al.* Convallatoxin promotes apoptosis and inhibits proliferation and angiogenesis through crosstalk between JAK2/STAT3 (T705) and mTOR/STAT3 (S727) signaling pathways in colorectal cancer. *Phytomedicine: Int. J. Phytotherapy Phytopharmacol.* **68**, 153172. <https://doi.org/10.1016/j.phymed.2020.153172> (2020).
- Kusaba, T. *et al.* Activation of STAT3 is a marker of poor prognosis in human colorectal cancer. *Oncol. Rep.* **15**(6), 1445–1451 (2006).
- Yue, Y., Zhang, Q., Wang, X. & Sun, Z. STAT3 regulates 5-Fu resistance in human colorectal cancer cells by promoting mcl-1-dependent cytoprotective autophagy. *Cancer Sci.* **114**(6), 2293–2305. <https://doi.org/10.1111/cas.15761> (2023).
- August, A. Who regulates whom: ZNF341 is an additional player in the STAT3/T(H)17 song. *Sci. Immunol.* <https://doi.org/10.1126/sciimmunol.aat9779> (2018).
- Cheng, Y. *et al.* KRAB zinc finger protein ZNF382 is a proapoptotic tumor suppressor that represses multiple oncogenes and is commonly silenced in multiple carcinomas. *Cancer Res.* **15**(16), 6516–6526. <https://doi.org/10.1158/0008-5472.can-09-4566> (2010).
- Wei, J. *et al.* The ubiquitin ligase TRAF6 negatively regulates the JAK-STAT signaling pathway by binding to STAT3 and mediating its ubiquitination. *PLoS One* **7**(11), e49567. <https://doi.org/10.1371/journal.pone.0049567> (2012).
- Wang, X. *et al.* HMGA2 facilitates colorectal cancer progression via STAT3-mediated tumor-associated macrophage recruitment. *Theranostics* **12**(2), 963–975. <https://doi.org/10.7150/thno.65411> (2022).
- Zhi, L. *et al.* SLC01B3 promotes colorectal cancer tumorigenesis and metastasis through STAT3. *Ageing* **15**(18), 22164–22175. <https://doi.org/10.18632/aging.203502> (2021).

22. Liang, J. *et al.* Transcription factor ZNF263 enhances EGFR-targeted therapeutic response and reduces residual disease in lung adenocarcinoma. *Cell. Rep.* **27**(2), 113771. <https://doi.org/10.1016/j.celrep.2024.113771> (2024).
23. Tuli, H. S. *et al.* STAT signaling as a target for intervention: From cancer inflammation and angiogenesis to non-coding RNAs modulation. *Mol. Biology Rep.* **49**(9), 8987–8999. <https://doi.org/10.1007/s11033-022-07399-w> (2022).
24. Verhoeven, Y. *et al.* The potential and controversy of targeting STAT family members in cancer. *Seminars Cancer Biol.* **60**, 41–56. <https://doi.org/10.1016/j.semcancer.2019.10.002> (2020).
25. Dorard, C. *et al.* RAF1 contributes to cell proliferation and STAT3 activation in colorectal cancer independently of microsatellite and KRAS status. *Oncogene* **42**(20), 1649–1660. <https://doi.org/10.1038/s41388-023-02683-w> (2023).
26. Schulz-Heddergott, R. *et al.* Therapeutic ablation of gain-of-function mutant p53 in colorectal cancer inhibits Stat3-mediated tumor growth and invasion. *Cancer Cell.* **13**(2), 298–314e7. <https://doi.org/10.1016/j.ccell.2018.07.004> (2018).
27. Hashemi, M. *et al.* STAT3 as a newly emerging target in colorectal cancer therapy: Tumorigenesis, therapy response, and pharmacological/nanoplatform strategies. *Environ. Res.* **15**, 116458. <https://doi.org/10.1016/j.envres.2023.116458> (2023).
28. Laudisi, F. *et al.* Progranulin sustains STAT3 hyper-activation and oncogenic function in colorectal cancer cells. *Mol. Oncol.* **13**(10), 2142–2159. <https://doi.org/10.1002/1878-0261.12552> (2019).
29. Wang, S. *et al.* NF- κ B activator 1 downregulation in macrophages activates STAT3 to promote adenoma-adenocarcinoma transition and immunosuppression in colorectal cancer. *BMC Med.* **29**(1), 115. <https://doi.org/10.1186/s12916-023-02791-0> (2023).
30. Hu, F. *et al.* The autophagy-independent role of BECN1 in colorectal cancer metastasis through regulating STAT3 signaling pathway activation. *Cell. Death Dis.* **1**(5), 304. <https://doi.org/10.1038/s41419-020-2467-3> (2020).
31. Rokavec, M. *et al.* IL-6R/STAT3/miR-34a feedback loop promotes EMT-mediated colorectal cancer invasion and metastasis. *J. Clin. Invest.* **124**(4), 1853–1867. <https://doi.org/10.1172/jci73531> (2014).
32. Jiang, H., Ge, H., Shi, Y., Yuan, F. & Yue, H. CAFs secrete CXCL12 to accelerate the progression and cisplatin resistance of colorectal cancer through promoting M2 polarization of macrophages. *Med. Oncol. (Northwood, London, England)*. **40**(3), 90. <https://doi.org/10.1007/s12032-023-01953-7> (2023).
33. Mneimneh, A. T., Darwiche, N. & Mehanna, M. M. Investigating the therapeutic promise of drug-repurposed-loaded nanocarriers: A pioneering strategy in advancing colorectal cancer treatment. *Int. J. Pharm.* **16**, 124473. <https://doi.org/10.1016/j.ijpharm.2024.124473> (2024).
34. Yadav, B. K., Patel, R., Prajapati, B. & Patel, G. Cutting-edge advances in nanocarrier-facilitated topical drug delivery systems for targeted skin cancer therapy: A comprehensive review. *Curr. Pharm. Biotechnol.* <https://doi.org/10.2174/0113892010312939240704141630> (2024).
35. Ma, L. *et al.* Mulberry leaf lipid nanoparticles: A naturally targeted CRISPR/Cas9 oral delivery platform for alleviation of colon diseases. *Small (Weinheim Der Bergstrasse Germany)* **20**(25), e2307247. <https://doi.org/10.1002/sml.202307247> (2024).
36. Issa, I. I. *et al.* CRISPR-Cas9 knockout screens identify DNA damage response pathways and BTK as essential for cisplatin response in diffuse large B-Cell lymphoma. *Cancers* <https://doi.org/10.3390/cancers16132437> (2024).

Author contributions

Y.D. and M.D. designed the study; Y.D. and Y.C. performed the experiments. Z.Y. and J.Y. provided critical samples and technical support. Y.D. drafted the paper. Z.Y. and M.D. revised the manuscript. All authors reviewed the manuscript.

Funding

This work was supported by the National Natural Science Foundation of China (No:82160588), the Gansu Natural Science Foundation (No:21JR1RA016, No:21JR7RA598) and the Gansu Youth Natural Science Foundation (No: 21JR7RA645, No:21JR7RA646).

Declarations

Competing interests

The authors declare no competing interests.

Ethical approval and consent to participate

Colorectal cancer tissues and adjacent normal tissues were collected and studied with the authorization and consent of colorectal cancer patients. The study protocol was approved by the Gansu Provincial Hospital Ethics Review Committee, No. 2024 – 300. The article does not contain any studies with animals performed by any of the authors. This study did not involve sensitive patient information, so it was exempted from the Gansu Provincial Hospital Ethics Review Committee.

Additional information

Supplementary Information The online version contains supplementary material available at <https://doi.org/10.1038/s41598-024-72636-0>.

Correspondence and requests for materials should be addressed to M.D.

Reprints and permissions information is available at www.nature.com/reprints.

Publisher's note Springer Nature remains neutral with regard to jurisdictional claims in published maps and institutional affiliations.

Open Access This article is licensed under a Creative Commons Attribution-NonCommercial-NoDerivatives 4.0 International License, which permits any non-commercial use, sharing, distribution and reproduction in any medium or format, as long as you give appropriate credit to the original author(s) and the source, provide a link to the Creative Commons licence, and indicate if you modified the licensed material. You do not have permission under this licence to share adapted material derived from this article or parts of it. The images or other third party material in this article are included in the article's Creative Commons licence, unless indicated otherwise in a credit line to the material. If material is not included in the article's Creative Commons licence and your intended use is not permitted by statutory regulation or exceeds the permitted use, you will need to obtain permission directly from the copyright holder. To view a copy of this licence, visit <http://creativecommons.org/licenses/by-nc-nd/4.0/>.

© The Author(s) 2024